Published OnlineFirst June 24, 2019; DOI: 10.1158/2326-6066.CIR-18-0875

Research Article

Cancer Immunology Research

Histone Deacetylase Inhibition Sensitizes PD1 Blockade–Resistant B-cell Lymphomas

Xiaoguang Wang[1], Brittany C. Waschke[1], Rachel A. Woolaver[1], Zhangguo Chen[1], Gan Zhang[2], Anthony D. Piscopio[3], Xuedong Liu[2,3], and Jing H. Wang[1]

Abstract

PD1 blockade is effective in a subset of patients with B-cell lymphoma (e.g., classical-Hodgkin lymphomas); however, most patients do not respond to anti-PD1 therapy. To study PD1 resistance, we used an isoform-selective histone deacetylase inhibitor (HDACi; OKI-179), and a mouse mature B-cell lymphoma, G1XP lymphoma, immunosuppressive features of which resemble those of human B-cell lymphomas, including downregulation of MHC class I and II, exhaustion of $CD8^+$ and $CD4^+$ tumor-infiltrating lymphocytes (TIL), and PD1-blockade resistance. Using two lymphoma models, we show that treatment of B-cell lymphomas refractory to PD1 blockade with both OKI-179 and anti-PD1 inhibited growth; furthermore, sensitivity to single or combined treatment required tumor-derived MHC class I, and positively correlated with MHC class II expression level. We conclude that OKI-179 sensitizes lymphomas to PD1-blockade by enhancing tumor immunogenicity. In addition, we found that different HDACis exhibited distinct effects on tumors and T cells, yet the same HDACi could differentially affect HLA expression on different human B-cell lymphomas. Our study highlights the immunologic effects of HDACis on antitumor responses and suggests that optimal treatment efficacy requires personalized design and rational combination based on prognostic biomarkers (e.g., MHCs) and the individual profiles of HDACi.

Introduction

Non-Hodgkin lymphomas (NHL) are a heterogeneous group of malignancies affecting lymphocytes. Collectively, NHL are the fifth most common cancers in the United States, and more than 90% of NHL are of B-cell origin (1). The standard treatment of NHL includes cytotoxic chemotherapy (cyclophosphamide, doxorubicin, vincristine) plus one steroid (prednisone) combined with mAb against CD20 (rituximab; R-CHOP; refs. 2, 3). For patients with diffuse large B-cell lymphoma (DLBCL), the most frequent type of NHL, the 10-year progression-free survival was 36.5% for R-CHOP; the rest of patients endure relapsed and/or refractory disease (4). PD1 blockade is effective in relapsed or refractory classical Hodgkin lymphomas and a subset of DLBCL (5, 6), however, most patients with B-cell lymphoma do not respond well to anti-PD1 (7). There are no good experimental models to study PD1 blockade resistance observed in human B-cell lymphomas. To address these issues, we employed a mouse mature B-cell lymphoma model, G1XP (8), which resembles human B-cell lymphomas, to test therapeutic strategies.

One mechanism mediating PD1 blockade resistance may be downregulation of MHC class I and II in tumors. MHC class I and II present peptides derived from self or foreign antigens to $CD8^+$ and $CD4^+$ T cells, respectively, thus, are essential for cancer cells to be recognized by antigen-specific $CD8^+$ and $CD4^+$ T cells. As such, down regulating MHCs reduces the immunogenicity of lymphomas. DLBCLs frequently harbor mutations or deletions inactivating β2-microglobulin (β2M; 29% of cases; ref. 9), an essential component of MHC class I complex, thereby preventing MHC class I expression on lymphomas. Apart from inactivating β_2M, additional undefined mechanisms result in the loss of MHC class I expression in >60% of DLBCL, suggesting that its selective loss during lymphomagenesis may mediate escape from immune surveillance (9). Diminished MHC class II expression also occurs frequently in DLBCLs and other types of mature B-cell lymphomas (10–15). MHC class II loss or low expression correlates with inferior survival in patients of DLBCL or classical Hodgkin lymphoma (10–12), or with poor prognosis in patients with DLBCL and primary mediastinal B-cell lymphoma (PMBCL) following chemotherapies (10, 16–18). Whether MHC expression influences the sensitivity of B-cell lymphomas to PD1 blockade remains unclear.

MHC class I downregulation also occurs in other types of cancers including colon, lung, and breast cancers (19–23). MHC class II loss correlated with a decrease of tumor-infiltrating T cells and an increase of metastatic potential of colorectal cancers (24). MHC class II expression serves as a favorable prognostic marker in colorectal carcinomas (25). Melanoma-specific MHC class II expression predicts response to anti-PD1/PD-L1 therapy (26). In contrast, mutations in the MHC class I pathway correlated with immune checkpoint inhibitor (ICI) resistance (27). Thus, restoring MHC class I and II expression on tumors has been suggested to benefit chemotherapy and immunotherapy (14, 22, 27). Reversible downregulation of MHC class I and class II, so-called "soft lesions," can be mediated by epigenetic modifications (23);

[1]Department of Immunology and Microbiology, University of Colorado, Anschutz Medical Campus, Aurora, Colorado. [2]Department of Biochemistry, University of Colorado Boulder, Boulder, Colorado. [3]OnKure Inc., Boulder, Colorado.

Note: Supplementary data for this article are available at Cancer Immunology Research Online (http://cancerimmunolres.aacrjournals.org/).

Corresponding Author: Jing H. Wang, University of Colorado, Anschutz Medical Campus, 12800 E. 19th Ave, Mail Stop 8333, Aurora, CO 80045. Phone: 303-724-8673; Fax: 303-724-4226; E-mail: jing.wang@ucdenver.edu

Cancer Immunol Res 2019;7:1318–31

doi: 10.1158/2326-6066.CIR-18-0875

Published OnlineFirst June 24, 2019; DOI: 10.1158/2326-6066.CIR-18-0875

moreover, "soft lesions" dominate MHC class I defects in human cancers (23, 28, 29). Most "soft lesions" of MHC class II are mediated by decreased histone acetylation rather than DNA hypermethylation (23, 28, 29).

Histone acetylation status is regulated by a dynamic equilibrium between histone acetyl transferases and histone deacetylases (HDAC). HDAC expression is often dysregulated in solid tumors and hematologic cancers, including B-cell lymphomas (30–33). Four FDA-approved HDAC inhibitors (HDACi), vorinostat, romidepsin, panobinostat, and belinostat, are used for treating hematologic cancers (34–36). Despite the success of these HDACis, each has liabilities including poor isoform selectivity, marginal potencies toward relevant isoforms, narrow therapeutic indices, and/or nonoral delivery routes. These drawbacks have spurred a search for alternatives with improved biological, physiochemical, and therapeutic properties. A natural product, largazole, was reported as a potent class I HDACi (37, 38); however, largazole has relatively poor physiochemical properties and is not amendable to large-scale chemical manufacturing. Thus, we initiated a lead optimization program resulting in the discovery of next-generation largazole derivatives OKI-005 and OKI-179 (39).

The efficacy of combining ICI with HDACis was tested previously in animal models or early-stage clinical studies (40–42). However, there are challenges in translating these observations into clinically useful therapeutics (43, 44). It remains poorly understood why combined ICI and HDACi worked in certain tumors but failed in others and what biomarkers can predict treatment efficacy. In addition, it remains poorly understood how HDACis affect the immunogenicity of cancer cells (44). To address these questions, we need syngeneic immunocompetent mouse models of B-cell lymphomas with altered immunogenicity. HDACis have been shown to recover or enhance expression of MHC class I and II in different types of cancers (28, 41, 45–49). However, it remains unknown whether HDACi sensitizes B-cell lymphomas to PD1 blockade by regulating MHC expression. Finally, although HDACi are known to modulate antitumor immunity, their net effects are dependent on the specific inhibitors used and the HDACs they target (50). It remains unknown what types of HDACi are suitable for combination with ICI.

In this study, we employed an HDACi (OKI-179) and G1XP lymphoma (8), created by lineage-specific deletion of a DNA repair gene, *Xrcc4*, and *Trp53* in germinal center (GC) B cells, because most human mature B-cell lymphomas are derived from GC or post-GC B cells (51). We show that G1XP lymphomas downregulated their MHC expression and resisted anti-PD1. We dissected the mechanisms by which the HDACi OKI-179 sensitizes the resistant lymphomas to anti-PD1.

Materials and Methods

In vivo treatment of lymphomas, tumor dissociation, and flow cytometry

Littermate controls of G1XP or BALB/c mice (6–8 weeks) were injected subcutaneously at both flanks with 1×10^6 G1XP or A20 lymphoma cells. When tumor size reached 200 to 350 mm^3, recipient mice were randomized into 4 groups and treated three times every other day with vehicle control (intraperitoneal injection of PBS and oral gavage of 0.1 mol/L citrate buffer), anti-PD1 (10 mg/kg/dose; BioXcell) via intraperitoneal injection, OKI-179 (60 mg/kg/dose) via oral gavage, or both anti-PD1 and OKI-179. When tumor size reached 2 cm in any dimension or other humane endpoints were met (e.g., necrotic tumors), mice were euthanized in accordance with institutional guidelines. Mice were maintained under specific pathogen–free conditions in the vivarium facility of University of Colorado Anschutz Medical Campus (Aurora, CO). Animal work was approved by the Institutional Animal Care and Use Committee (IACUC) of University of Colorado Anschutz Medical Campus (Aurora, CO).

Tumors were harvested from tumor-bearing mice. Tumor weight was measured before dissociation and tumors were processed into single-cell suspension. Tumor-infiltrating lymphocytes (TIL) were stained with antibodies against CD45, B220, CD3, TCRβ, CD4, CD8, and CD69. Antibodies used for flow cytometry were listed in Supplementary Table S1. Dead cells were excluded by Live/Dead Fixable Green Dead Cell Stain Kit (Invitrogen). BD Fix/Permeabilization buffer was used for intracellular staining of IFNγ and granzyme B in TILs. Equal numbers of tumors were cultured *in vitro* for 6 hours in the presence of 50 ng/mL phorbol 12-myristate 13-acetate (Sigma-Aldrich), 1 μg/mL ionomycin (Sigma-Aldrich), and 5 μg/mL BFA (BioLegend). Data were acquired on BD Fortessa or BD FACSCalibur and analyzed with FlowJo software V10.

Cell culture

G1XP lymphomas were generated, established, and cultured as described previously (8). A20 lymphoma cells were obtained from cell line vendor ATCC in 2017. OCI-LY1, OCI-LY3, OCI-LY7, and SU-DHL-16 were obtained from Dr. Wing C. (John) Chan (City of Hope Medical Center, Duarte, CA) in 2016 and cultured as described previously (52). The cell line authentication and *Mycoplasma* testing were performed by Molecular Biology Service Center at the Barbara Davis Center (University of Colorado, Anschutz Medical Campus, Aurora, CO) in 2019. The cells were tested and reauthenticated by PCR assays as described (http://www.barbaradaviscenter.org/). The number of passages between thawing and use in the described experiments ranged from two to five.

Lymphoma cells were cultured at 0.5×10^6/mL and treated with vehicle control, OKI-005, or OKI-179 at indicated concentrations for 24 or 48 hours. Cells in triplicates were treated as described above, fixed in 70% ethanol, and stained with PI and anti-pH3 as described previously (52). Cell cycles were determined by flow cytometry (FL1-H/FL2-A). Splenic T cells were isolated from wt B6-naïve mice by Negative Selection Kit (Stemcell Technologies), cultured with mouse T-Activator CD3/CD28 Dynabeads (Thermo Fisher Scientific), and collected 3 days after culture for flow cytometry analysis. Murine primary B cells were isolated from spleens of syngeneic mice by negative selection kit (Stemcell Technologies), cultured with mouse IL4 (20 ng/mL) and anti-CD40 (1 μg/mL) as described previously (53) and collected 4 days after culture for flow cytometry or OKI-179 treatment. Human primary B cells were isolated from human cord blood by negative selection kit (Stemcell Technologies), cultured with IL4 (10 ng/mL), IL21 (10 ng/mL), and anti-CD40 (1 μg/mL) and collected 5 days after culture for flow cytometry.

RNA-seq, Western blot, and cell-cycle analysis

G1XP, OCI-Ly7, and murine primary B cells were treated with 500 nmol/L of OKI-179 for 16 hours, respectively, and total

Published OnlineFirst June 24, 2019; DOI: 10.1158/2326-6066.CIR-18-0875

RNA was isolated by TRIzol (Roche). Isolated RNA was subject to library preparation and sequenced with Illumina NovaSEQ 6000 platform by the genomic core facility at University of Colorado Anschutz Medical Campus (Aurora, CO). Primary antibodies used in Western blot analysis were listed in Supplementary Table S1. Secondary horseradish peroxidase–conjugated anti-mouse and anti-rabbit were purchased from Jackson ImmunoResearch. Protein bands were developed by ECL Western blotting detection reagents (GE Healthcare) according to kit instructions. Cell cycles were determined as described previously (52).

B2M knockout by CRISPR-Cas9 and H2-K1 transfection

Guide RNA (gRNA) oligos targeting mouse *B2M* gene were designed by online software (http://crispr.mit.edu/). Four gRNA oligos were synthesized and annealed to generate two DNA fragments (1-For 5′-caccgAGTATACTCACGCCACCCAC-3′, 1-Rev 5′-aaacGTGGGTGGCGTGAGTATACTc-3′; 2-For 5′-caccgCGTATGTATCAGTCTCAGTG-3′, 2-Rev 5′-aaacCACTGAGACTGATACATACGc-3′). The two DNA fragments were cloned into pX458 vector, respectively, according to the protocol described previously (54). Both newly constructed pX458 plasmids were cotransfected into G1XP or A20 lymphomas with Nucleofector Kit V (Lonza). Single clones lacking MHC class I were screened by flow cytometry with an anti-mouse MHC class I antibodies and confirmed by PCR with primers (SF 5′-TTATCCAGAGTAGAAATGGAACAGGG-3′, SR 5′-GTATTCTCTAACAATCTCAGTATGC-3′). Deleted fragments were cloned into pGEM-T vector (Promega) and sequenced by MCLAB. G1XP B2M$^{-/-}$ lymphoma harbored a deletion on each allele of B2M gene, respectively (deletion on allele 1: 3211–3219, 3381–3401; allele 2: 3214–3222, 3386–3406 of B2M genomic DNA, NC_000068.7: 122147687-122153082, total length of 5396 bp). A20 B2M$^{-/-}$ lymphoma cells harbored the same deletion on both alleles of the B2M gene (deletion location: 3394–3571; NC_000068.7:122147687-122153082, total length of 5396 bp).

Total RNA was isolated from G1XP lymphomas, and used for cDNA synthesis with a Reverse Transcription Kit (Promega). *H2-K1* cDNA was amplified by PCR with primers (For 5′-GACAGAATTCATGGTACCGTGCACGCTGC-3′; Rev 5′-GCAGTCTAGATCACG CTAGAGAATGAGGGT-3′). The amplified *H2-K1* fragment was subcloned into pcDNA3.1(+) vector. The newly constructed pcDNA3.1(+) plasmid was transfected into G1XP lymphomas using Mouse B Cell Nucleofector Kit (Lonza). After culturing for 2 days, transfected cells were selected with 600 μg/mL neomycin until neomycin-resistant foci were identified. Single G1XP clones with varied MHC class I or II expression were identified by flow cytometry.

Results

Biochemical profile and pharmacokinetics of OKI-179

Our efforts toward the discovery of a largazole-derived HDACi were prompted by the lackluster physiochemical properties and synthetic challenges of largazole (55, 56). These efforts resulted in the invention of OKI-005 and OKI-179 (39), first- and second-generation prodrug candidates, respectively, derived from the same parent thiol congener. IC_{50} values were obtained with OKI-179 thiol (the active parent form of OKI-179 and OKI-005) under cell-free, biochemical assay conditions using purified enzymes, compared favorably with other HDACi (Supplementary Table S2). OKI-179 thiol inhibits class I, IIb, and IV HDACs (Supplementary Table S2).

To determine the pharmacokinetics of OKI-179 *in vivo*, OKI-179 was administered to mice via oral gavage. OKI-179 converted to its active metabolite rapidly in murine plasma, with similar pharmacokinetic profiles observed in both female and male mice (Supplementary Fig. S1A–S1D). Maximum concentration (C_{max}) in male and female mice ranged from 337 to 4,980 ng/mL (Supplementary Fig. S1A). The time to reach C_{max} *in vivo* (T_{max}) was 0.083 hours (for dose of 25 mg/kg) and 0.25 hours (for dose of 50 mg/kg and 100 mg/kg). The half-life [$t_{1/2}$(h)] is shown in Supplementary Fig. S1D. On the basis of C_{max} *in vivo*, we decided to use the following concentrations of OKI for *in vitro* treatment: 250 nmol/L, 500 nmol/L, and 1 μmol/L.

OKI treatment leads to cell-cycle arrest, apoptosis, and growth inhibition in tumors

HDACi treatment is cytotoxic to cancer cells (57). To examine whether OKI-005 or OKI-179 exhibits cytotoxic effects on tumors, G1XP lymphomas were treated with OKI-005 or OKI-179 *in vitro*. Both OKI-005 and OKI-179 inhibited the growth of G1XP lymphomas in a dose-dependent manner (Fig. 1A). OKI-179 treatment arrested tumor cells at G_0–G_1 phases and reduced the percentage of cells at S-phase (Supplementary Fig. S2A and S2B). To test the effects of OKI on mitotic entry, we assessed the phosphorylation of histone3 (pH3), which serves as a marker for M-phase entry because chromosome condensation requires H3 phosphorylation. We found that pH3 was reduced upon treatment of OKI-179 (Fig. 1B and C) and OKI-005 (Supplementary Fig. S2C and S2D), demonstrating OKI-treated lymphomas were inhibited for M-phase progression. Finally, cleaved caspase-3 production, a marker for apoptosis, was induced in G1XP lymphomas upon treatment of OKI-179 (Fig. 1D–F) and OKI-005 (Supplementary Fig. S2E and S2F). Overall, OKI-005 and OKI-179 inhibit tumor cell growth by inducing cell-cycle arrest and apoptosis.

OKI-179 and OKI-005 are congeners because they have identical drug structures but different prodrug structures. OKI-179 is designed to have better drug exposure *in vivo* and better pharmaceutical quality in terms of chemistry, manufacturing, and controls. OKI-179 was developed on the basis of OKI-005 and is more suitable for *in vivo* studies. OKI-179 received IND approval from FDA and entered phase I clinical trials in 2019. Thus, we employed OKI-179 for subsequent analyses because it will be more translatable to clinical settings.

OKI-179 sensitizes G1XP lymphomas to PD1 blockade

We transplanted G1XP lymphomas (8) into syngeneic wild-type (WT) recipient mice that developed secondary tumors approximately 2 weeks after inoculation. We harvested secondary tumors and analyzed TILs. Both $CD8^+$ and $CD4^+$ TILs upregulated PD1 compared with control splenic T cells (Fig. 1G). PD1 is a coinhibitory receptor associated with T-cell exhaustion, suggesting that G1XP lymphomas might be sensitive to anti-PD1 treatment. We inoculated WT recipients with G1XP lymphomas, when tumor size reached about 250 to 350 mm^3, we randomized recipient mice into four groups and treated them with vehicle control, anti-PD1, OKI-179, or OKI-179 plus anti-PD1 (combo). We harvested tumors on day 21 after inoculation for TIL analysis (short-term; Fig. 1H and I) or observed the cohorts for tumor growth (long-term; Fig. 1J and K). In both scenarios, anti-PD1

Published OnlineFirst June 24, 2019; DOI: 10.1158/2326-6066.CIR-18-0875

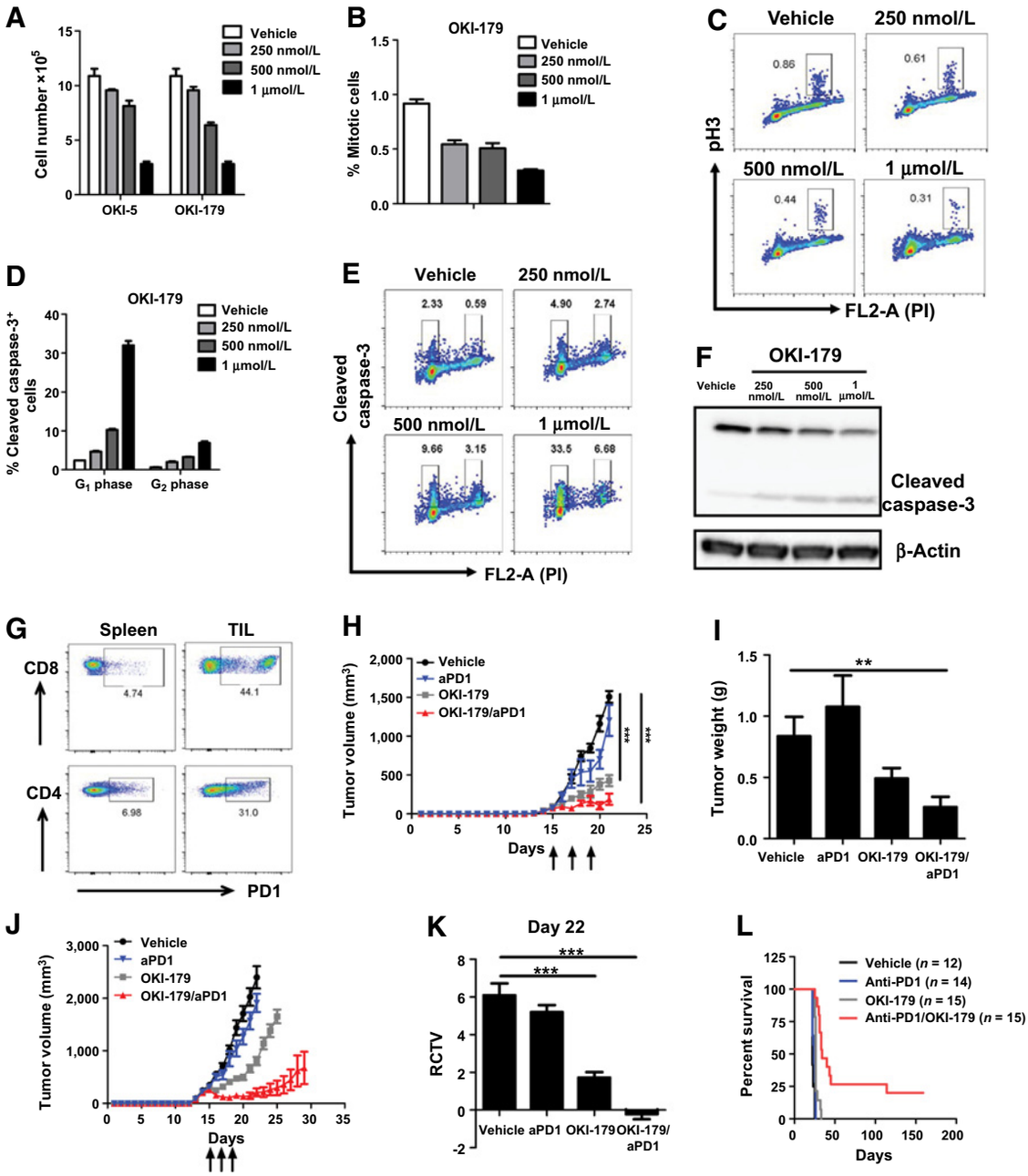

Figure 1.

G1XP lymphomas resisted anti-PD1 and were sensitized by OKI-179 to anti-PD1. **A,** OKI-005 or OKI-179 treatment inhibited G1XP lymphoma proliferation. Cell numbers in triplicates were counted. **B** and **C,** OKI-179 treatment reduced mitotic entry of G1XP lymphomas. Cells in triplicates were treated as in **A**, fixed, and stained with PI and anti-pH3. Cell cycles were determined by flow cytometry. **D** and **E,** OKI-179 treatment induced apoptosis of G1XP lymphomas. Cells in triplicates were treated as in **A**, fixed, and stained for PI and cleaved caspase-3. The percentage of apoptotic cells were determined by flow cytometry. **F,** Apoptosis of G1XP lymphomas upon OKI-179 treatment. Cells were treated as described in **A**. Caspase-3 was detected by Western blot analysis and β-actin as the loading control. Data are representative results of two independent experiments for **A–F**. **G,** Immunosuppressive phenotypes of TILs in the transplanted G1XP lymphomas. Tumors were harvested 15 days after inoculation and TILs or splenocytes (as control) were analyzed by flow cytometry. **H** and **I,** Tumor growth of G1XP lymphomas upon different treatments. G1XP lymphomas were transplanted into syngeneic recipient mice, and tumor-bearing mice (tumor sizes between 250–350 mm^3) were randomized into 4 groups and treated with vehicle control, OKI-179, anti-PD1 or both, respectively, on day 15, 17, and 19 after tumor inoculation. Tumor sizes were measured daily ($n = 6$ per group; **H**). Tumor weights were measured on day 21 after tumor inoculation (**I**) and subsequently used for TIL analysis. **J** and **K,** Long-term tumor growth of G1XP lymphomas upon different treatments (**J**) and relative change in tumor volume (RCTV) on day 22 (**K**). Mice were treated as described in **H**, vehicle ($n = 12$), anti-PD-1 ($n = 14$), OKI-179 ($n = 16$), and OKI-179/anti-PD1 ($n = 14$). Data are representative results of three independent experiments for **G–K**. **L,** Kaplan–Meier curve of G1XP lymphoma-bearing recipients. Mice were treated as described in **H**. Data are combined from three independent experiments for **L**. Statistical significance was calculated with one-way ANOVA, Tukey multiple comparison test (**, $P < 0.01$; ***, $P < 0.001$).

Published OnlineFirst June 24, 2019; DOI: 10.1158/2326-6066.CIR-18-0875

failed to suppress G1XP lymphoma growth (Fig. 1H–K). OKI-179 alone showed an inhibitory effect on G1XP lymphoma growth at early time points, whereas combo treatment inhibited tumor growth (Fig. 1H–K). When data were analyzed together from three independent experiments in which treated recipients were monitored up to 168 days after tumor inoculation, approximately 25% of the recipients from combo group survived, whereas all other control groups were terminated (according to IACUC guideline) or died due to tumor growth (Fig. 1L). These data show that G1XP lymphomas resist anti-PD1, and OKI-179 treatment sensitizes lymphomas to anti-PD1.

MHC downregulation in G1XP lymphomas and OKI-mediated MHC upregulation

To reveal the mechanisms of PD1 blockade resistance, we tested whether G1XP lymphomas downregulated their MHCs. We established several G1XP lymphoma lines and found that G1XP lymphomas downregulated MHC class I expression compared with activated primary B cells (Fig. 2A, left), which were used as controls because they mimic the developmental stage of G1XP lymphomas. MHC class II expression on G1XP lymphomas was also reduced compared with activated primary B cells (Fig. 2A, right). G1XP lymphomas expressed less MHC class I or class II than other mouse B-cell lymphoma lines, such as CH12 and A20 (Fig. 2B). We conclude that G1XP lymphomas provide a model for studying tumors with reduced immunogenicity.

MHC downregulation can be reversible or irreversible. We tested our HDACis, OKI-179 and OKI-005, for their ability to affect MHC expression on G1XP lymphomas. Lymphomas were cultured in the presence of OKI-179, OKI-005, or vehicle control, and both OKI-179 and OKI-005 upregulated MHC class I and class II expression in a dose-dependent manner *in vitro* (Fig. 2C; Supplementary Fig. S3). To test whether OKI-179 treatment affects MHC class I and II expression on G1XP lymphomas *in vivo*, we inoculated G1XP lymphomas into syngeneic recipient mice. Tumor-bearing recipients were randomized into four groups and treated as described above. OKI-179 or OKI-179/anti-PD1 treatment caused lymphomas to upregulate MHC class I and class II *in vivo* (Fig. 2D–F). These data indicate that OKI-179 increases the immunogenicity of cancer cells. Downregulation of MHC class I and II in G1XP lymphomas was reversible; thus, it likely occurs via epigenetic mechanisms.

OKI-179 and OKI-179/anti-PD1 treatment activated TILs in G1XP lymphomas

Because of the increased MHC expression on G1XP lymphomas upon OKI-179 treatment, we tested whether the treatment influences $CD8^+$ and $CD4^+$ TILs. Tumors were harvested from recipients treated with vehicle control, OKI-179, anti-PD1 or combo, respectively. We isolated tumors and TILs and performed flow cytometry analysis 21 days after tumor inoculation. This time point was chosen because control group usually had to be terminated due to the size of tumors exceeding institutional guideline. We also cultured the TILs for 6 hours, then examined IFNγ production in $CD4^+$ and $CD8^+$ TILs and granzyme B in $CD8^+$ TILs. Combo treatment increased the percentage and number of $CD4^+$ (Fig. 3A–C) and $CD8^+$ TILs (Fig. 3D–F). Furthermore, combo treatment activated TILs and increased IFNγ production in both $CD4^+$ (Fig. 3G and H) and $CD8^+$ TILs (Fig. 3I and J) and granzyme B production in $CD8^+$ TILs (Fig. 3K and L). OKI-179 treatment alone also increased IFNγ production in both $CD4^+$ and $CD8^+$ TILs (Fig. 3G and I). Combo treatment also induced CD69 expression in both $CD4^+$ (Supplementary Fig. S4A and S4B) and $CD8^+$ TILs (Supplementary Fig. S4C and S4D). Thus, combined OKI-179/anti-PD1 treatment promoted $CD4^+$ and $CD8^+$ TIL activation.

Sensitivity of G1XP lymphomas to treatment affected by MHC expression

To determine whether tumor-derived MHC class I is required for efficacy of combo treatment, we employed the CRISPR/Cas9 technique to delete the *B2M* gene in G1XP lymphoma. Deletion of the *B2M* gene was confirmed by PCR and Sanger sequencing (Fig. 4A). Consistently, MHC class-I was absent in G1XP $B2M^{-/-}$ lymphoma (Fig. 4B). WT G1XP lymphoma clone was transplanted into recipient mice that were treated as described above and exhibited sensitivity to single OKI-179 or combo treatment (Fig. 4C), similar to what was observed in parental G1XP lymphomas. However, single OKI-179 or combo treatment did not inhibit the growth of G1XP $B2M^{-/-}$ lymphomas (Fig. 4D). These data show that tumor-derived MHC class I is essential for the efficacy of combo and single OKI-179 treatment.

Next, we investigated whether OKI-179-mediated MHC class I upregulation is sufficient, namely, whether OKI-179 renders lymphomas sensitive to anti-PD1 just by upregulating MHC class I in lymphomas. We ectopically re-expressed MHC class I in G1XP lymphomas and tested whether tumor's sensitivity to anti-PD1 is affected by the amount of reintroduced MHC class I. We choose to ectopically reexpress H2-K1, an MHC class I α chain gene, in G1XP lymphomas, because H2-K1 is one of the most abundantly expressed MHC class I alleles and OKI-179 significantly upregulated H2-K1 expression in G1XP lymphomas (Supplementary Fig. S5A). Stable clones were selected that expressed more or less MHC class I (Fig. 4E).

Comparing with MHC class I^{low} clone (E8), MHC class I^{high} clone (C10) expressed more MHC class I but showed similar MHC class II expression *in vitro* and *in vivo* (Fig. 4E; Supplementary Fig. S5B). However, clone E8 and C10 were equally insensitive to anti-PD1 (Fig. 4F and G). These data suggest that upregulation of MHC class I is not sufficient for rendering tumors sensitive to PD1 blockade. In addition, we compared the MHC class II expression among different G1XP lymphoma clones, and found that clone D1 presented more MHC class II expression than E8 and C10, but low MHC class I expression *in vitro* and *in vivo* (Fig. 4E; Supplementary Fig. S5B). Anti-PD1 treatment significantly inhibited the growth of clone D1 (Fig. 4H). Our data indicate that more MHC class II correlates with greater tumor sensitivity to PD1 blockade.

A20 lymphoma response to treatment requires tumor-derived MHC class I

To further test whether treatment efficacy of OKI-179 or anti-PD1 is dependent on MHC class I, we employed the A20 lymphoma model known to express high amounts of both MHC class I and II (Fig. 2B). We transplanted A20 lymphomas into syngeneic recipient mice (WT Balb/c) and found that $CD8^+$ and $CD4^+$ TILs upregulated PD1 compared with control splenic T cells (Fig. 5A). Single OKI-179 or anti-PD1 treatment significantly increased recipient survival (Fig. 5B) and inhibited tumor growth (Fig. 5C). Although combo treatment appeared

Published OnlineFirst June 24, 2019; DOI: 10.1158/2326-6066.CIR-18-0875

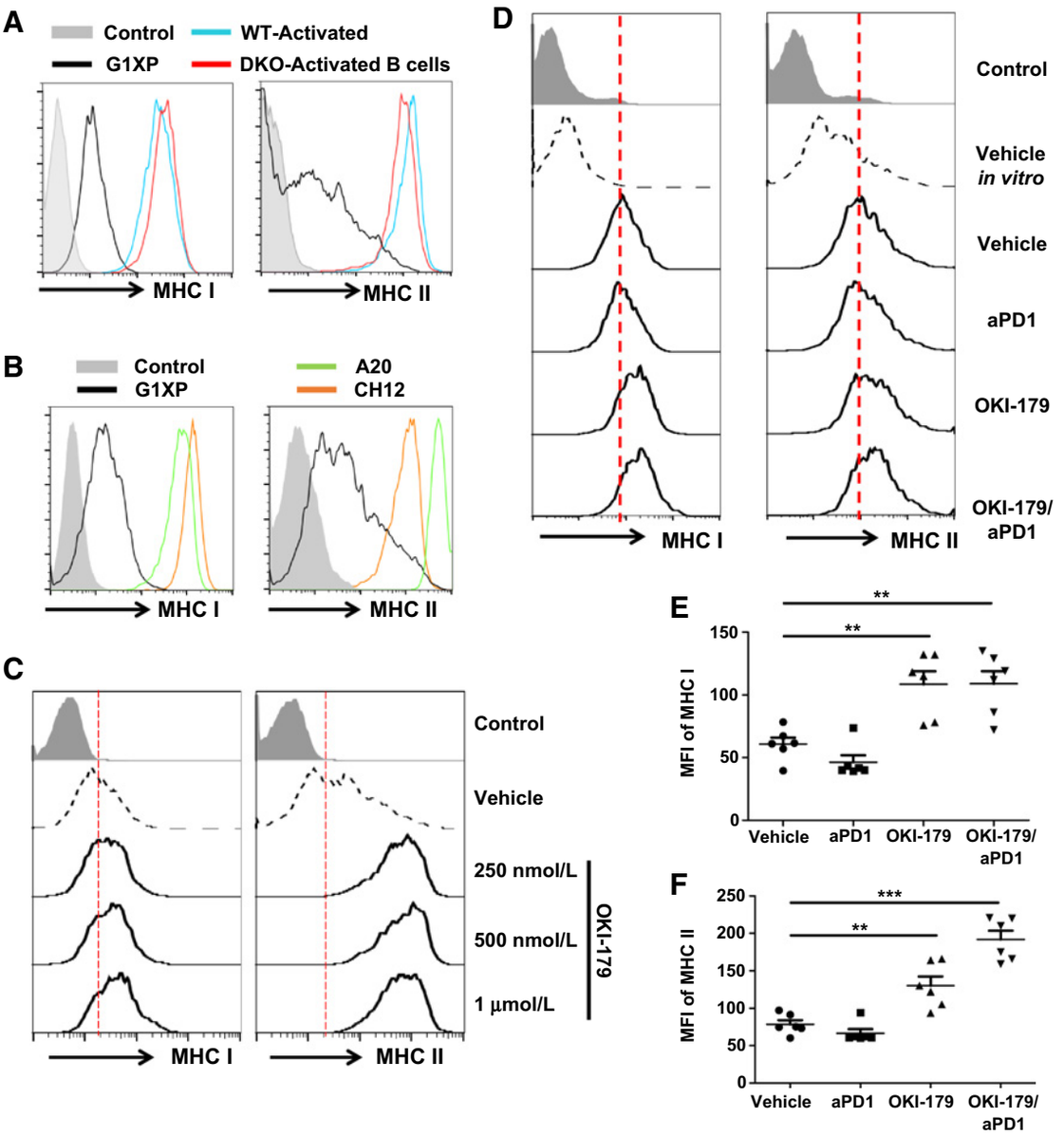

Figure 2.

G1XP lymphomas downregulated MHC class I and class II that could be upregulated by OKI-179. **A** and **B,** Downregulation of MHC class I and II in G1XP lymphomas compared with activated primary B cells (**A**) and other murine B-cell lymphomas (**B**). Cells were stained with anti-mouse MHC class I or class II and analyzed by flow cytometry. **C,** OKI-179 treatment upregulated MHC class I and II in G1XP lymphomas *in vitro*. G1XP lymphomas were cultured with vehicle control or OKI-179 for 48 hours. **D–F,** OKI-179 treatment upregulated MHC class I and II in G1XP lymphoma *in vivo*. Tumor-bearing recipients were treated as described above on day 15 and tumors were harvested on day 17 after inoculation. Dead cells were excluded and MHC class I or class II expression was determined by flow cytometry (**D**) and median fluorescence intensity (MFI) was shown (**E** and **F**). Statistical significance was calculated with one-way ANOVA, Tukey multiple comparison test (**, $P < 0.01$; ***, $P < 0.001$). Representative data are shown from three independent experiments.

to be more effective, no significant differences were detected between single and combo treatment (Fig. 5B and C). Thus, our data suggest that the high immunogenicity of A20 lymphomas correlates with high sensitivity to monotherapies or combo treatment.

To test the role of MHC class I in A20 lymphoma model, we generated B2M-KO A20 lymphomas using CRISPR/Cas9 approach (Supplementary Fig. S6A). A20 B2M$^{-/-}$ lymphoma cells harbored the same deletion on both alleles of the *B2M* gene (Supplementary Fig. S6A). Because of saturated expression of MHC class I and II on A20 lymphoma, OKI-179 had no effect on MHC class I and II expression (Supplementary Fig. S6B). OKI-179 was unable to induce the expression of MHC class I on A20 B2M$^{-/-}$ lymphoma (Supplementary Fig. S6C). A20 B2M$^{-/-}$ lymphomas were transplanted into syngeneic recipient mice that were treated as described above. In contrast to A20 WT

Published OnlineFirst June 24, 2019; DOI: 10.1158/2326-6066.CIR-18-0875

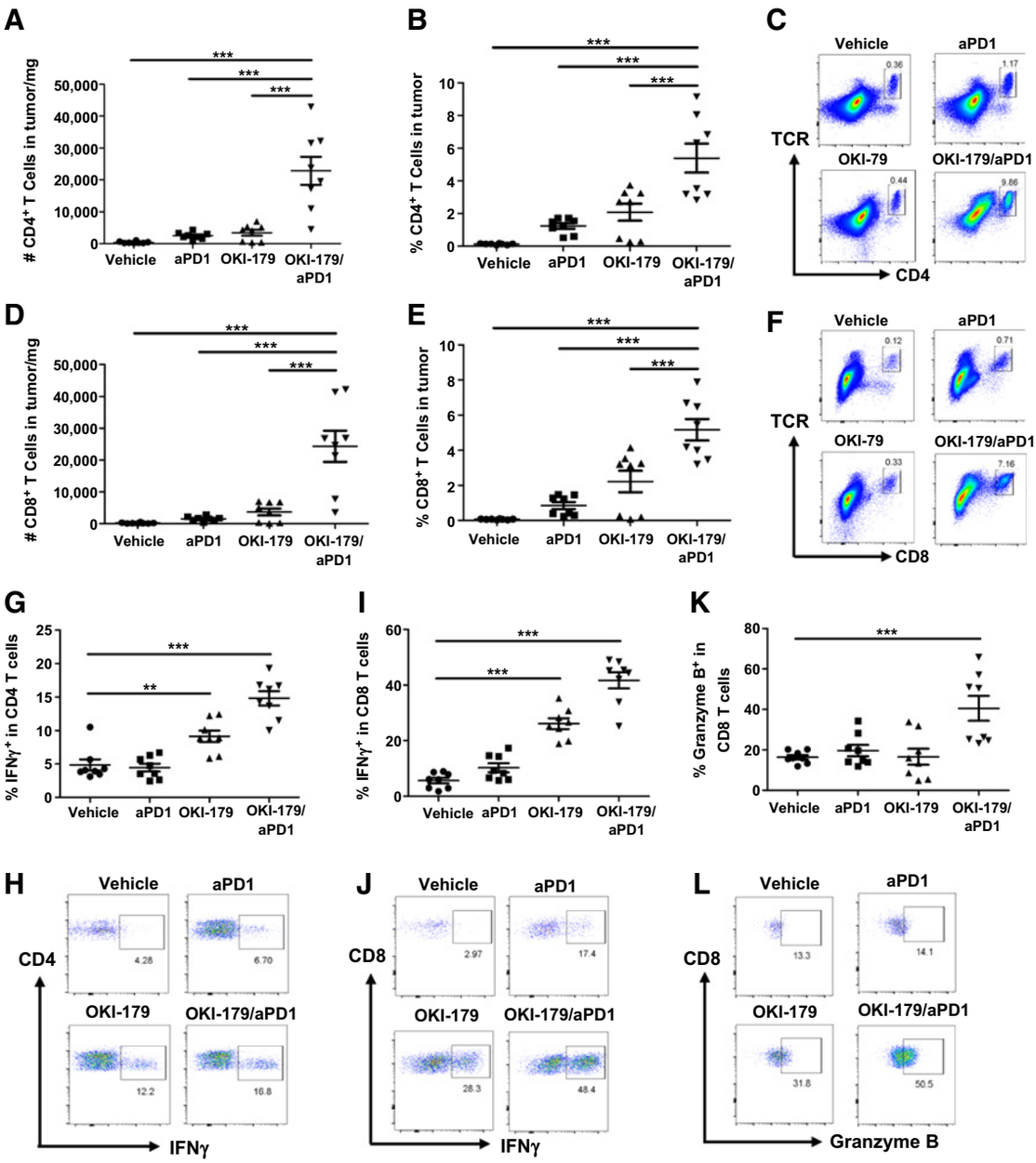

Figure 3.

Combined treatment of OKI-179/anti-PD1 increased and activated CD4$^+$ and CD8$^+$ TILs in G1XP lymphomas. Tumor-bearing recipients were treated as indicated, on day 15, 17, and 19 after tumor inoculation. Tumors were harvested on day 21 after inoculation ($n = 8$ per group). **A–F,** Cells were stained and analyzed by flow cytometry. Numbers (**A**), percentages (**B**), and representative plots (**C**) of CD4$^+$ TILs in G1XP lymphoma. Numbers (**D**), percentages (**E**), and representative plots (**F**) of CD8$^+$ TILs in G1XP lymphoma. **G–L,** Harvested tumors were stimulated with PMA/ionomycin for 6 hours *in vitro* and analyzed by flow cytometry. Percentages (**G**) and representative plots (**H**) of IFNγ$^+$CD4$^+$ T cells in total CD4$^+$ TILs. Percentages (**I**) and representative plots (**J**) of IFNγ$^+$CD8$^+$ T cells in total CD8$^+$ TILs. Percentages (**K**) and representative plots (**L**) of granzyme B$^+$CD8$^+$ T cells in total CD8$^+$ TILs. Data were combined from two independent experiments. Statistical significance was calculated with one-way ANOVA, Tukey multiple comparison test (**, $P < 0.01$; ***, $P < 0.001$).

lymphomas, A20 B2M$^{-/-}$ lymphomas were resistant to single or combined treatment of OKI-179 and anti-PD1 (Fig. 5D and E). These data demonstrate that the sensitivity of tumor cells to OKI-179 or anti-PD1 treatment requires tumor-derived MHC class I expression. OKI-179 treatment inhibited proliferation and mitotic entry of A20 WT and B2M$^{-/-}$ lymphomas (Supplementary Fig. S7A–S7F), and induced apoptosis of A20 WT lymphomas (Supplementary Fig. S7G). However, the treatment effects of OKI-179 were abolished in A20 B2M$^{-/-}$ lymphomas (Fig. 5E), demonstrating that OKI-179's efficacy depends on its immunoregulatory effects instead of direct cytotoxic effects.

Published OnlineFirst June 24, 2019; DOI: 10.1158/2326-6066.CIR-18-0875

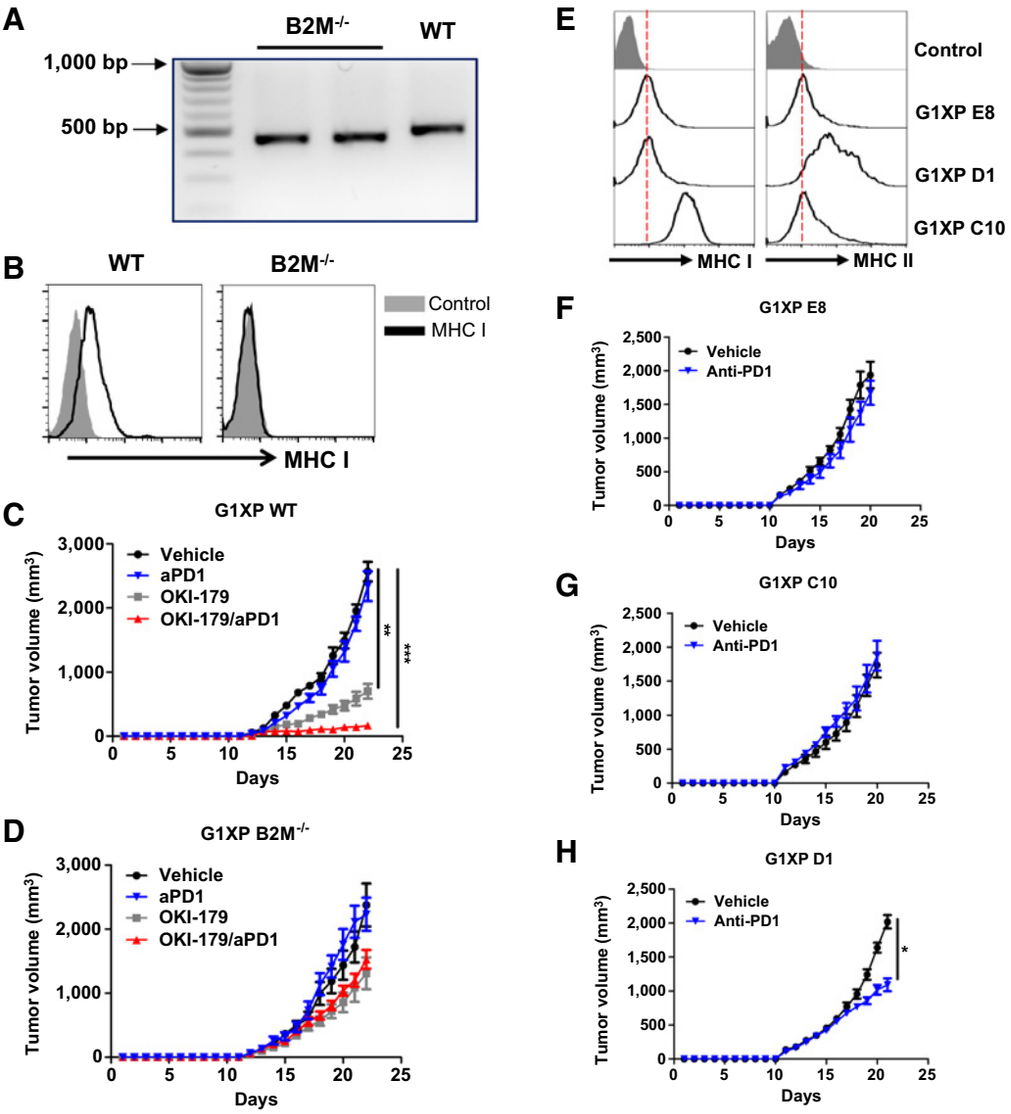

Figure 4.

Sensitivity of G1XP lymphomas to treatment was affected by MHC expressions. **A** and **B,** Deletion of *β2M* gene resulted in the absence of MHC class I expression in G1XP lymphoma. **A,** PCR products of WT versus *β2M*-deleted clones. **B,** Representative plot of WT or $\beta2M^{-/-}$ G1XP lymphomas. **C** and **D,** Elimination of the therapeutic effects of OKI-179 on G1XP lymphomas by *β2M* deletion. Recipient mice harboring WT (**C**) or $\beta2M^{-/-}$ (**D**) G1XP lymphomas were randomized into 4 groups and treated as indicated on day 13, 15, and 17 after tumor inoculation when tumor size reached 100–200 mm^3. Tumor size was measured daily ($n = 6$–10 per group). Data are representative results of two independent experiments for **C** and **D**. **E,** Ectopic expression of MHC class I in G1XP lymphomas. H2-K1 was ectopically expressed in G1XP lymphomas by transfection. Single clones were obtained that exhibited variable expression of MHC class I and II: clone E8 (MHC-I^{low}, MHC-II^{low}), C10 (MHC-I^{high}, MHC-II^{low}) and D1 (MHC-I^{low}, MHC-II^{high}). Tumor growth of G1XP lymphoma clone E8 (**F**), C10 (**G**) and D1 (**H**) upon anti-PD1 treatment. Tumor-bearing recipients were randomized into two groups and treated with vehicle control and anti-PD1, respectively, on day 11, 13, and 15 after tumor inoculation when tumor size reached 100–200 mm^3. Tumor size was measured daily ($n = 12$ per group). Data were combined from two independent experiments. Statistical significance was calculated with unpaired *t* test or one-way ANOVA (*, $P < 0.05$; **, $P < 0.01$; ***, $P < 0.001$).

Variable effects of HDACi on T-cell proliferation and MHC class I induction

To test whether different HDACi have varied effects on T-cell proliferation and activation, we purified T cells and stimulated them with anti-CD3/anti-CD28 beads in the presence of vehicle control or increasing concentration of HDACi for 3 days *in vitro*. OKI-179 and vorinostat did not affect the proliferation of $CD4^+$ or $CD8^+$ T cells (Fig. 6A and B; Supplementary Fig. S8A). However, panobinostat inhibited both $CD4^+$ and $CD8^+$ T-cell proliferation (Fig. 6C and D). OKI-179 and vorinostat had no effect on IFNγ production by $CD4^+$ or $CD8^+$ T cells (Supplementary Fig. S8B and S8C).

To determine whether other HDACi also induce MHC class I, we compared vorinostat with OKI-179 at the same dose range, and found that no induction of MHC class I occurred with vorinostat up to 1 μmol/L, whereas OKI-179 had a steady

Published OnlineFirst June 24, 2019; DOI: 10.1158/2326-6066.CIR-18-0875

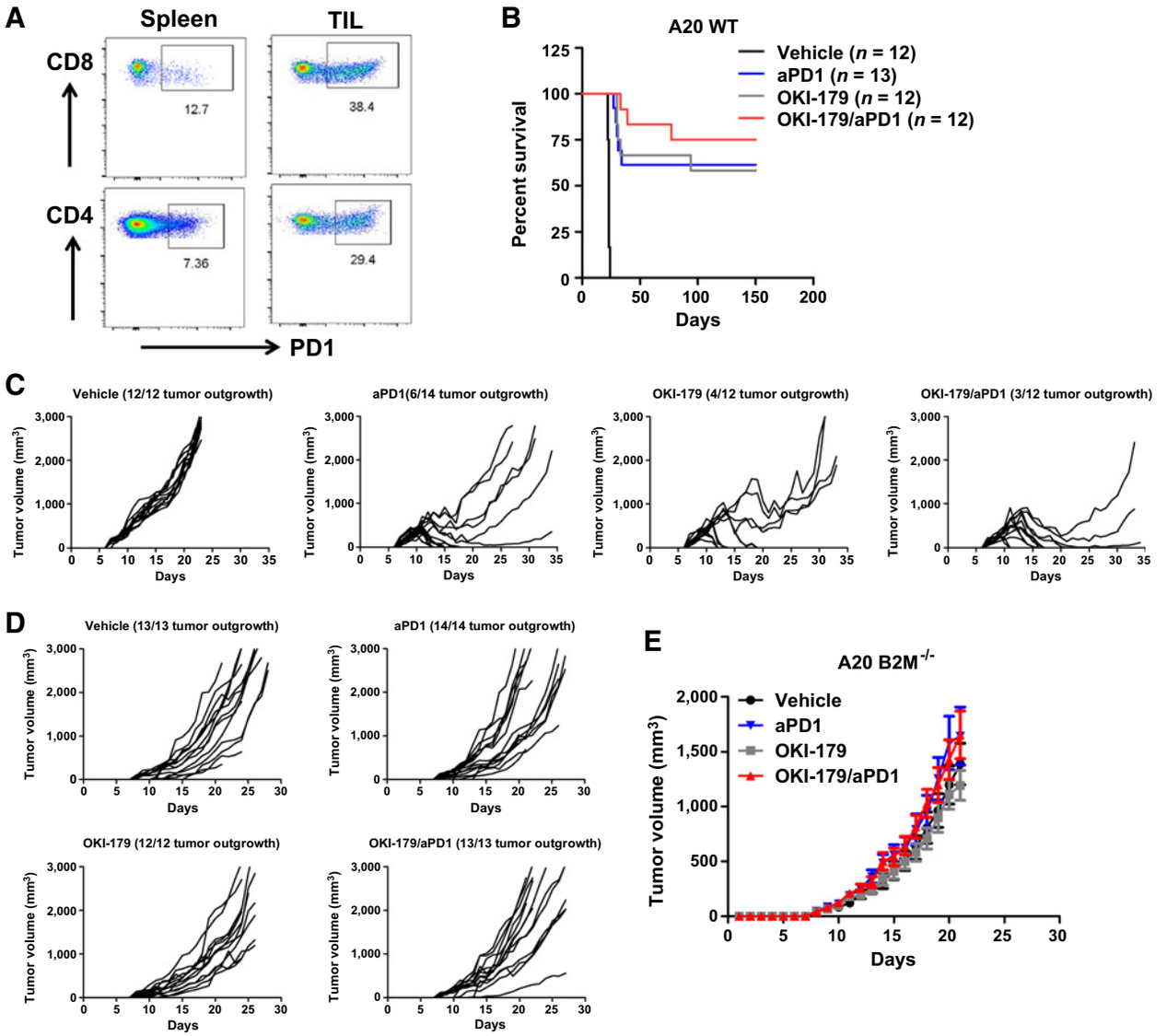

Figure 5.

Sensitivity of A20 lymphomas to treatment requires MHC class I. **A,** Immunosuppressive phenotypes of TILs in the transplanted A20 lymphomas. WT BALB/c mice were injected with A20 lymphomas. Tumors were harvested 15 days after inoculation and TILs or splenocytes (as control) were analyzed. **B,** Kaplan–Meier curve of recipient mice inoculated with A20 lymphomas. Tumor-bearing mice were randomized into 4 groups and treated with vehicle ($n = 12$), OKI-179 ($n = 12$), anti-PD1 ($n = 13$), or both ($n = 12$) on day 9, 11, and 13 after tumor inoculation (tumor size ~200 mm^3). Data were combined from two independent experiments. Log-rank (Mantel–Cox) test, vehicle versus anti-PD1: $P < 0.001$; vehicle versus OKI-179: $P < 0.001$; anti-PD1 versus combo: $P = 0.3544$; OKI-179 versus combo: $P = 0.3305$. **C,** Tumor growth of A20 WT lymphomas upon different treatments. Tumor-bearing recipients were treated as described in **B** when tumor size reaches 200 mm^3. Tumor size was measured daily ($n = 12$ or 14 per group). Representative data are shown from two independent experiments. **D** and **E,** Tumor growth of A20 B2M$^{-/-}$ lymphomas upon different treatments. Recipient mice harboring A20 B2M$^{-/-}$ lymphomas were treated as described in **B** on day 11, 13, and 15 after tumor inoculation (tumor size ~200 mm^3). Tumor size was measured daily and data are combined from two independent experiments ($n = 12$–14 per group). Individual or combined tumor growth is shown in **D** or **E**, respectively.

dose-dependent increase (Fig. 6E). Vorinostat induced less expression of MHC class II than OKI-179 (Fig. 6F). This is probably due to the fact that vorinostat is not as potent in HDAC inhibition as OKI-179 (Supplementary Table S2). Panobinostat has a comparable class I HDAC inhibition potency to OKI-179 (Supplementary Table S2) and it can induce MHC class I and II expressions similarly to OKI-179 (Supplementary Fig. S8D). We conclude that different HDACi exhibit variable effects on T cells and tumors, suggesting that not all HDACis are suitable for combination with PD1 blockade.

OKI-179 enhances expression of PD-L1 and human HLA on tumor cells

PD-L1$^+$ cancers might be more sensitive to PD1 blockade (58, 59), such as Hodgkin lymphomas with PD-L1 amplification (6, 60, 61), suggesting that PD-L1 upregulation may serve

Published OnlineFirst June 24, 2019; DOI: 10.1158/2326-6066.CIR-18-0875

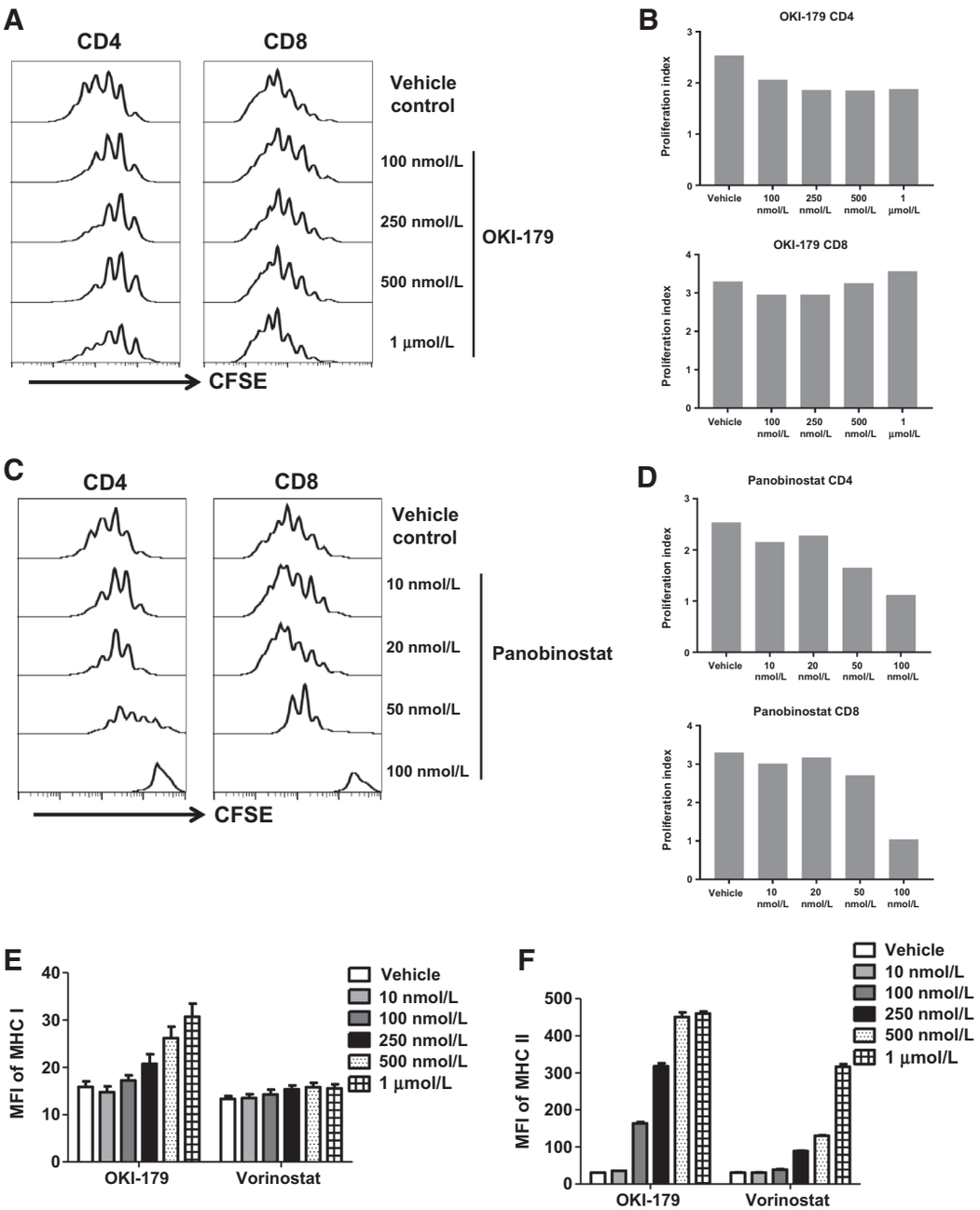

Figure 6.

Different HDACi exhibit distinct effects on T cells and tumors. **A–D,** Effects of OKI-179 and panobinostat on T-cell proliferation. CFSE-labeled T cells were activated with anti-CD3/anti-CD28 in the presence of vehicle control or OKI-179 (**A** and **B**) or panobinostat (**C** and **D**) for 72 hours. Panobinostat inhibited T-cell proliferation at higher concentrations, whereas OKI-179 did not affect T-cell proliferation. Proliferation index was calculated using FlowJo proliferation analysis program for $CD4^+$ and $CD8^+$ T cells treated with vehicle or OKI-179 (**B**) or panobinostat (**D**). Representative data are shown from three independent experiments for **A–D**. **E** and **F,** OKI-179 upregulated MHC expression on G1XP lymphomas more than vorinostat. G1XP lymphomas were cultured with OKI-179 (**E**) or vorinostat (**F**) for 48 hours. Cells were stained and analyzed by flow cytometry. Representative MFI data are shown from two independent experiments.

as a biomarker to predict PD1 blockade sensitivity. Our RNA-Seq data showed that OKI-179 treatment also upregulated PD-L1 expression in both G1XP and OCI-Ly7 lymphomas (Fig. 7A and B). However, OKI-179 had no effect on PD-L1 expression in activated primary mouse B cells (Fig. 7C). Furthermore, PD-L1 expression was upregulated in G1XP lymphomas by OKI-179 in a dose-dependent manner (Fig. 7D). In contrast, the expression of costimulatory factors, including CD83, CD86, OX40L and CD137L, were not altered by OKI-005 or OKI-179 (Supplementary Fig. S9A–S9D). OKI-179 inhibited the growth of human B-

Published OnlineFirst June 24, 2019; DOI: 10.1158/2326-6066.CIR-18-0875

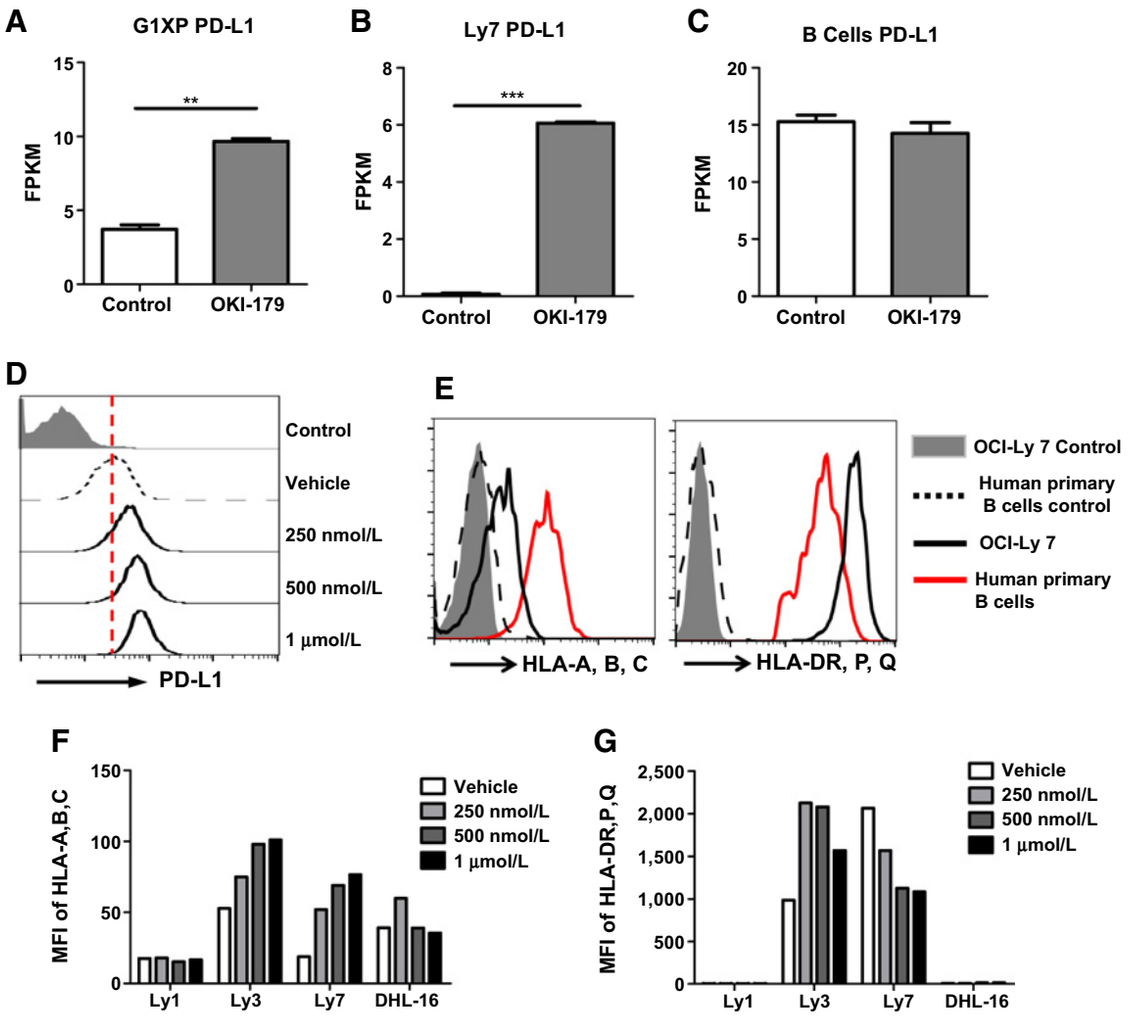

Figure 7.

OKI-179 upregulated PD-L1 in murine and human B-cell lymphomas and affected MHC expressions of different human B-cell lymphomas. **A–C,** Increased transcription of PD-L1 in G1XP and OCI-Ly7 lymphomas upon OKI-179 treatment. G1XP lymphomas (**A**), OCI-Ly7 (**B**), and activated primary B cells (**C**) were cultured with vehicle control or OKI-179 for 16 hours. **D,** Upregulation of PD-L1 in G1XP lymphoma upon OKI-179 treatment. G1XP lymphomas were cultured with vehicle control or OKI-179 for 48 hours. Cells were stained and analyzed by flow cytometry. **E,** Downregulation of HLA-A, B, and C in OCI-Ly7 lymphoma compared with activated human primary B cells. **F** and **G,** Different regulations of HLA in human B-cell lymphomas upon OKI-179 treatment. Various human B-cell lymphoma lines were cultured with vehicle control or OKI-179 for 24 hours. Lymphomas were stained and analyzed by flow cytometry. Representative data are shown from two independent experiments. Statistical significance was calculated with unpaired *t* test (**, $P < 0.01$; ***, $P < 0.001$).

cell lymphoma lines in a dose-dependent manner (Supplementary Fig. S10).

To establish a general concept of OKI-179-mediated MHC upregulation, we treated various human B-cell lymphoma lines with OKI-179. Human OCI-Ly7 lymphomas downregulated their HLA-A, B, and C but not HLA-DP, DQ, and DR compared with human primary B cells (Fig. 7E). OKI-179 treatment enhanced the expression of HLA-A, B, and C in OCI-Ly3 and OCI-Ly7, whereas OKI-179 had no effect on OCI-Ly1 and little effect on SU-DHL-16 cell line (Fig. 7F). OKI-179 upregulated HLA-DP, DQ, and DR in OCI-Ly3 cells, but not in OCI-Ly1, OCI-Ly7, and SU-DHL-16 cells (Fig. 7G). Thus, we conclude that different human B-cell lymphoma lines respond differently to OKI-179 treatment in terms of MHC upregulation.

Discussion

We tested the therapeutic efficacy of combined OKI-179/anti-PD1 treatment and found that: (i) OKI-179 sensitizes G1XP lymphomas to anti-PD1 by enhancing tumor immunogenicity; (ii) sensitivity to single or combined treatment required tumor-derived MHC class I and positively correlated with MHC class II expression in tumors; (iii) the durable antitumor effects of OKI-179 depend on antigen-specific $CD8^+$ T-cell-mediated immune responses; and (iv) different HDACis exhibited distinct effects on tumors and T cells, yet the same HDACi could differentially affect HLA expression in different human B-cell lymphomas. Thus, our studies highlight immunologic effects of HDACis on antitumor responses and suggest that optimal treatment efficacy requires personalized design

Published OnlineFirst June 24, 2019; DOI: 10.1158/2326-6066.CIR-18-0875

and rational combination based on prognostic biomarkers (e.g., MHCs) and individual profiles of HDACis.

Human B-cell lymphomas often downregulate MHC expression (9–15) and resist anti-PD1 (7). Lacking proper models hinders our effort to understand the underlying mechanisms of these observations. G1XP lymphoma is a syngeneic mouse model for mature B-cell lymphoma that downregulates MHCs and resists anti-PD1. This model provides an opportunity to elucidate how altering lymphoma immunogenicity influences cancer immunotherapy outcome. Different lymphomas responded differentially to single anti-PD1 treatment, with a correlation to their MHC expression. For instance, MHC high–expressing A20 lymphomas are sensitive to anti-PD1, whereas MHC low–expressing G1XP lymphomas resist anti-PD1. Consistently, acquired resistance to PD1 blockade associates with deletional mutation in the *B2M* gene in a relapse sample of a patient with melanoma (62). PD1 blockade–resistant tumors downregulated MHC class I in a murine lung cancer model (63). Although tumor-derived MHC class I is essential for sensitivity to single or combo treatment, increasing MHC class I alone did not render tumors sensitive to anti-PD1. In contrast, higher expression of tumor-derived MHC class II correlated with increased sensitivity to anti-PD1. Studies show that therapeutic effects of PD1 blockade correlate with the expression of MHC class II but not MHC class I in patients with melanoma (26, 64). Collectively, these studies suggest that sensitivity to PD1 blockade needs high MHC class II expression.

MHC downregulation in G1XP lymphomas is reversible and rescued by epigenetic agents, such as HDACi. However, OKI-179 is unable to restore irreversible MHC class I downregulation in B-cell lymphomas. When tumor-derived MHC class I is removed genetically, the therapeutic effects of single OKI-179 or combo treatment were abolished. Thus, we consider OKI-179 to be a personalized drug suitable for treating tumors with reversible MHC downregulation. We suggest that MHC expression might serve as a predictive biomarker for treatment efficacy of OKI-179. Aside from classical MHC class I, B2M is also required for expression of other nonclassical MHC molecules such as H2-M5 (65), involvement of which we cannot rule out. However, our RNA-seq data did not detect changes in the B2M-associated molecules upon OKI-179 treatment, suggesting that these nonclassical MHC class I molecules are not necessary for mediating responses to OKI-179.

HDACis modulate antitumor immunity (43). For instance, anticancer effects of vorinostat require immune system (66, 67). However, not all HDACis are created equal and their net effects are dependent on the specific inhibitors used and the HDACs they target (44, 50). Typically, inhibitors are developed on the basis of on-target activity; however, off-target activity could result in undesirable side effects or toxicity. For example, panobinostat and romidepsin are potent HDACis but are also toxic. The narrow window for therapeutic success makes such HDACis unsuitable for combined therapies with ICIs. Pan-HDACi such as vorinostat target all 11 HDACs, which is problematic because class IIa HDACs have opposing functions to class I HDACs in modulating immune responses (e.g., Treg; ref. 68). In addition, not all HDACis are equally potent at reprogramming cancer epigenome. For example, vorinostat did not upregulate MHC class I in G1XP tumors. A large dose of vorinostat will be needed to achieve MHC class I induction *in vivo*, quite a challenge given its poor drug metabolism and pharmacokinetics profile. Thus, when interpreting the immunologic effects of HDACis, we must be aware of the dose, cellular context, and selectivity of agents, and the impact of HDACi on both tumors and T cells.

OKI-179 has favorable properties compared with previously reported HDACis, with its selectivity, oral availability with a broad therapeutic window, direct inhibition of B-cell lymphoma proliferation, and no toxic effects on T-cell proliferation and activation, providing improved therapeutic effects due to its potent immune-enhancing activity. OKI-179 can also effectively inhibit HDAC3, which has been implicated in regulating MHC class II expression in B-cell lymphomas (69). Thus, OKI-179 is a promising agent for treating cancers with reversible MHC downregulation, such as B-cell lymphomas.

OKI-179 upregulates PD-L1 in G1XP and human B-cell lymphomas. PD-L1 interacts with PD1 expressed on $CD4^+$ and $CD8^+$ TILs, thereby leading to inhibition of effector functions and exhaustion of T cells (70). To overcome the detrimental effects of OKI-179–mediated PD-L1 upregulation on antitumor immunity, anti-PD1 needs to be employed together with OKI-179. Indeed, combo treatment more effectively inhibits B-cell lymphomas, providing a rationale for developing combinatorial therapy using epigenetic agents and ICIs. HDACis also upregulate PD-L1 and augment therapeutic efficiency of PD1 blockade in melanoma (71) or lung cancers (42), suggesting the applicability of such combined strategies to other types of cancers.

$PD\text{-}L1^+$ cancers might be more sensitive to PD1 blockade (58, 59). PMBCL and Hodgkin lymphomas harbor recurrent chromosomal translocations or amplifications of PD-L1 and PD-L2, leading to overexpression of PD-L1 and PD-L2 (60, 61). Consistently, Hodgkin lymphomas are very sensitive to PD1 blockade. Clinical trials of PD1 therapy showed promising results in PMBCL (6, 72). These data suggest that PD-L1 upregulation may serve as a biomarker to predict combo treatment sensitivity. Prior studies show that tumor-derived PD-L1 is not required for the efficacy of anti-PD-L1 treatment because host cells still express PD-L1 (73). It remains to be determined whether altering tumor-derived PD-L1 will affect the efficacy of combo treatment in our B-cell lymphoma model. On the other hand, HDACi-mediated PD-L1 upregulation may explain why these agents generally fail to treat cancers as a single agent. Our studies may provide insights into why HDACis alone failed and why there should be a renewed emphasis on the effects of HDACi on PD-L1 upregulation.

Disclosure of Potential Conflicts of Interest

G. Zhang is a board member, has ownership interest (including stock, patents, etc.), and is a consultant/advisory board member for OnKure. A.D. Piscopio has ownership interest (including stock, patents, etc.) in OnKure. X. Liu is an officer, has ownership interest (including stock, patents, etc.), and is a consultant/advisory board member for OnKure. No potential conflicts of interest were disclosed by the other authors.

Authors' Contributions

Conception and design: X. Wang, G. Zhang, X. Liu, J.H. Wang
Development of methodology: X. Wang, J.H. Wang
Acquisition of data (provided animals, acquired and managed patients, provided facilities, etc.): X. Wang, B.C. Waschke, R.A. Woolaver, G. Zhang, J.H. Wang
Analysis and interpretation of data (e.g., statistical analysis, biostatistics, computational analysis): X. Wang, B.C. Waschke, R.A. Woolaver, A.D. Piscopio, J.H. Wang

Published OnlineFirst June 24, 2019; DOI: 10.1158/2326-6066.CIR-18-0875

Writing, review, and/or revision of the manuscript: X. Wang, B.C. Waschke, Z. Chen, A.D. Piscopio, X. Liu, J.H. Wang
Administrative, technical, or material support (i.e., reporting or organizing data, constructing databases): Z. Chen, A.D. Piscopio
Study supervision: Z. Chen, J.H. Wang
Other (supplied test article): A.D. Piscopio

Acknowledgments

We thank Stephanie Cung, Amanda M. Perras, and Erin Kitten for technical help. We apologize to those whose work was not cited due to length restrictions. This work was supported by University of Colorado School of Medicine and Cancer Center Startup Funds (to J.H. Wang), R21-CA184707, R21-AI110777, R01-CA166325, R21-AI133110, and R01-CA229174 (to J.H. Wang), a fund from Cancer League of Colorado and American Cancer Society (ACS IRG #16-184-56; to Z. Chen), R01GM113141 and R01AR068254 (to X. Liu). R.A. Woolaver is supported by a NIH F31 Fellowship (F31DE027854). X. Wang is supported by an AAI Careers in Immunology Fellowship.

The costs of publication of this article were defrayed in part by the payment of page charges. This article must therefore be hereby marked *advertisement* in accordance with 18 U.S.C. Section 1734 solely to indicate this fact.

Received December 7, 2018; revised March 22, 2019; accepted June 13, 2019; published first June 24, 2019.

References

1. Scott DW, Gascoyne RD. The tumour microenvironment in B cell lymphomas. Nat Rev Cancer 2014;14:517–34.
2. Vose JM, Link BK, Grossbard ML, Czuczman M, Grillo-Lopez A, Gilman P, et al. Phase II study of rituximab in combination with chop chemotherapy in patients with previously untreated, aggressive non-Hodgkin's lymphoma. J Clin Oncol 2001;19:389–97.
3. Czuczman MS, Grillo-Lopez AJ, White CA, Saleh M, Gordon L, LoBuglio AF, et al. Treatment of patients with low-grade B-cell lymphoma with the combination of chimeric anti-CD20 monoclonal antibody and CHOP chemotherapy. J Clin Oncol 1999;17:268–76.
4. Coiffier B, Thieblemont C, Van Den Neste E, Lepeu G, Plantier I, Castaigne S, et al. Long-term outcome of patients in the LNH-98.5 trial, the first randomized study comparing rituximab-CHOP to standard CHOP chemotherapy in DLBCL patients: a study by the Groupe d'Etudes des Lymphomes de l'Adulte. Blood 2010;116:2040–5.
5. Armand P, Nagler A, Weller EA, Devine SM, Avigan DE, Chen YB, et al. Disabling immune tolerance by programmed death-1 blockade with pidilizumab after autologous hematopoietic stem-cell transplantation for diffuse large B-cell lymphoma: results of an international phase II trial. J Clin Oncol 2013;31:4199–206.
6. Ansell SM, Lesokhin AM, Borrello I, Halwani A, Scott EC, Gutierrez M, et al. PD-1 blockade with nivolumab in relapsed or refractory Hodgkin's lymphoma. N Engl J Med 2015;372:311–9.
7. Goodman A, Patel SP, Kurzrock R. PD-1-PD-L1 immune-checkpoint blockade in B-cell lymphomas. Nat Rev Clin Oncol 2017;14:203–20.
8. Chen Z, Elos MT, Viboolsittiseri SS, Gowan K, Leach SM, Rice M, et al. Combined deletion of Xrcc4 and Trp53 in mouse germinal center B cells leads to novel B cell lymphomas with clonal heterogeneity. J Hematol Oncol 2016;9:2.
9. Challa-Malladi M, Lieu YK, Califano O, Holmes AB, Bhagat G, Murty VV, et al. Combined genetic inactivation of beta2-Microglobulin and CD58 reveals frequent escape from immune recognition in diffuse large B cell lymphoma. Cancer Cell 2011;20:728–40.
10. Rimsza LM, Roberts RA, Miller TP, Unger JM, LeBlanc M, Braziel RM, et al. Loss of MHC class II gene and protein expression in diffuse large B-cell lymphoma is related to decreased tumor immunosurveillance and poor patient survival regardless of other prognostic factors: a follow-up study from the Leukemia and Lymphoma Molecular Profiling Project. Blood 2004;103:4251–8.
11. Roberts RA, Wright G, Rosenwald AR, Jaramillo MA, Grogan TM, Miller TP, et al. Loss of major histocompatibility class II gene and protein expression in primary mediastinal large B-cell lymphoma is highly coordinated and related to poor patient survival. Blood 2006;108:311–8.
12. Diepstra A, van Imhoff GW, Karim-Kos HE, van den Berg A, te Meerman GJ, Niens M, et al. HLA class II expression by Hodgkin Reed-Sternberg cells is an independent prognostic factor in classical Hodgkin's lymphoma. J Clin Oncol 2007;25:3101–8.
13. Prochazka V, Jarošová M, Prouzova Z, Nedomova R, Papajik T, Indrák K. Immune escape mechanisms in diffuse large B-cell lymphoma. ISRN Immunol 2012;2012:208903.
14. Nijland M, Veenstra RN, Visser L, Xu C, Kushekhar K, van Imhoff GW, et al. HLA dependent immune escape mechanisms in B-cell lymphomas: implications for immune checkpoint inhibitor therapy? Oncoimmunology 2017;6:e1295202.
15. de Charette M, Marabelle A, Houot R. Turning tumour cells into antigen presenting cells: the next step to improve cancer immunotherapy? Eur J Cancer 2016;68:134–47.
16. Rosenwald A, Wright G, Chan WC, Connors JM, Campo E, Fisher RI, et al. The use of molecular profiling to predict survival after chemotherapy for diffuse large-B-cell lymphoma. N Engl J Med 2002;346:1937–47.
17. Rimsza LM, Leblanc ML, Unger JM, Miller TP, Grogan TM, Persky DO, et al. Gene expression predicts overall survival in paraffin-embedded tissues of diffuse large B-cell lymphoma treated with R-CHOP. Blood 2008;112:3425–33.
18. Rimsza LM, Farinha P, Fuchs DA, Masoudi H, Connors JM, Gascoyne RD. HLA-DR protein status predicts survival in patients with diffuse large B-cell lymphoma treated on the MACOP-B chemotherapy regimen. Leuk Lymphoma 2007;48:542–6.
19. Rooney MS, Shukla SA, Wu CJ, Getz G, Hacohen N. Molecular and genetic properties of tumors associated with local immune cytolytic activity. Cell 2015;160:48–61.
20. Lawrence MS, Stojanov P, Mermel CH, Robinson JT, Garraway LA, Golub TR, et al. Discovery and saturation analysis of cancer genes across 21 tumour types. Nature 2014;505:495–501.
21. Campbell JD, Alexandrov A, Kim J, Wala J, Berger AH, Pedamallu CS, et al. Distinct patterns of somatic genome alterations in lung adenocarcinomas and squamous cell carcinomas. Nat Genet 2016;48:607.
22. Garrido F, Aptsiauri N, Doorduijn EM, Garcia Lora AM, van Hall T. The urgent need to recover MHC class I in cancers for effective immunotherapy. Curr Opin Immunol 2016;39:44–51.
23. Garrido F, Cabrera T, Aptsiauri N. "Hard" and "soft" lesions underlying the HLA class I alterations in cancer cells: implications for immunotherapy. Int J Cancer 2010;127:249–56.
24. Warabi M, Kitagawa M, Hirokawa K. Loss of MHC class II expression is associated with a decrease of tumor-infiltrating T cells and an increase of metastatic potential of colorectal cancer: immunohistological and histopathological analyses as compared with normal colonic mucosa and adenomas. Pathol Res Pract 2000;196:807–15.
25. Sconocchia G, Eppenberger-Castori S, Zlobec I, Karamitopoulou E, Arriga R, Coppola A, et al. HLA class II antigen expression in colorectal carcinoma tumors as a favorable prognostic marker. Neoplasia 2014;16:31–42.
26. Johnson DB, Estrada MV, Salgado R, Sanchez V, Doxie DB, Opalenik SR, et al. Melanoma-specific MHC-II expression represents a tumour-autonomous phenotype and predicts response to anti-PD-1/PD-L1 therapy. Nat Commun 2016;7:10582.
27. Sharma P, Hu-Lieskovan S, Wargo JA, Ribas A. Primary, adaptive, and acquired resistance to cancer immunotherapy. Cell 2017;168:707–23.
28. Cycon KA, Mulvaney K, Rimsza LM, Persky D, Murphy SP. Histone deacetylase inhibitors activate CIITA and MHC class II antigen expression in diffuse large B-cell lymphoma. Immunology 2013;140:259–72.
29. Smahel M. PD-1/PD-L1 blockade therapy for tumors with downregulated MHC class I expression. Int J Mol Sci 2017;18:1331–44.
30. Zain J, O'Connor OA. Targeting histone deacetyalses in the treatment of B- and T-cell malignancies. Invest New Drugs 2010;28Suppl 1:S58–78.
31. Lee SH, Yoo C, Im S, Jung JH, Choi HJ, Yoo J. Expression of histone deacetylases in diffuse large B-cell lymphoma and its clinical significance. Int J Med Sci 2014;11:994–1000.

32. Ropero S, Esteller M. The role of histone deacetylases (HDACs) in human cancer. Mol Oncol 2007;1:19–25.
33. Lee JJ, Murphy GF, Lian CG. Melanoma epigenetics: novel mechanisms, markers, and medicines. Lab Invest 2014;94:822–38.
34. Yoon S, Eom GH. HDAC and HDAC inhibitor: from cancer to cardiovascular diseases. Chonnam Med J 2016;52:1–11.
35. Kelly WK, Marks P, Richon VM. CCR 20th Anniversary Commentary: vorinostat-gateway to epigenetic therapy. Clin Cancer Res 2015;21: 2198–200.
36. Marks PA. The clinical development of histone deacetylase inhibitors as targeted anticancer drugs. Expert Opin Investig Drugs 2010;19:1049–66.
37. Ying Y, Taori K, Kim H, Hong J, Luesch H. Total synthesis and molecular target of largazole, a histone deacetylase inhibitor. J Am Chem Soc 2008; 130:8455–9.
38. Taori K, Paul VJ, Luesch H. Structure and activity of largazole, a potent antiproliferative agent from the Floridian marine cyanobacterium Symploca sp. J Am Chem Soc 2008;130:1806–7.
39. Liu X, Phillips AJ, Ungermannova D, Nasveschuk CG, Zhang G, inventors; University of Colorado Boulder, assignee. Macrocyclic compounds useful as inhibitors of histone deacetylases. US Patent US8754050B2. 2014 Jun 17.
40. Patel SA, Minn AJ. Combination cancer therapy with immune checkpoint blockade: mechanisms and strategies. Immunity 2018;48:417–33.
41. Woods DM, Woan K, Cheng F, Wang H, Perez-Villarroel P, Lee C, et al. The antimelanoma activity of the histone deacetylase inhibitor panobinostat (LBH589) is mediated by direct tumor cytotoxicity and increased tumor immunogenicity. Melanoma Res 2013;23:341–8.
42. Zheng H, Zhao W, Yan C, Watson CC, Massengill M, Xie M, et al. HDAC inhibitors enhance T-cell chemokine expression and augment response to PD-1 immunotherapy in lung adenocarcinoma. Clin Cancer Res 2016;22: 4119–32.
43. Hull EE, Montgomery MR, Leyva KJ. HDAC inhibitors as epigenetic regulators of the immune system: impacts on cancer therapy and inflammatory diseases. BioMed Res Int 2016;2016:8797206.
44. Kroesen M, Gielen P, Brok IC, Armandari I, Hoogerbrugge PM, Adema GJ. HDAC inhibitors and immunotherapy; a double edged sword? Oncotarget 2014;5:6558–72.
45. Chou SD, Khan AN, Magner WJ, Tomasi TB. Histone acetylation regulates the cell type specific CIITA promoters, MHC class II expression and antigen presentation in tumor cells. Int Immunol 2005;17:1483–94.
46. Magner WJ, Kazim AL, Stewart C, Romano MA, Catalano G, Grande C, et al. Activation of MHC class I, II, and CD40 gene expression by histone deacetylase inhibitors. J Immunol 2000;165:7017–24.
47. Manning J, Indrova M, Lubyova B, Pribylova H, Bieblova J, Hejnar J, et al. Induction of MHC class I molecule cell surface expression and epigenetic activation of antigen-processing machinery components in a murine model for human papilloma virus 16-associated tumours. Immunology 2008;123:218–27.
48. Turner TB, Meza-Perez S, Londono A, Katre A, Peabody JE, Smith HJ, et al. Epigenetic modifiers upregulate MHC II and impede ovarian cancer tumor growth. Oncotarget 2017;8:44159–70.
49. Vo DD, Prins RM, Begley JL, Donahue TR, Morris LF, Bruhn KW, et al. Enhanced antitumor activity induced by adoptive T-cell transfer and adjunctive use of the histone deacetylase inhibitor LAQ824. Cancer Res 2009;69:8693–9.
50. McCaw TR, Randall TD, Forero A, Buchsbaum DJ. Modulation of antitumor immunity with histone deacetylase inhibitors. Immunotherapy 2017; 9:1359–72.
51. Kuppers R. Mechanisms of B-cell lymphoma pathogenesis. Nat Rev Cancer 2005;5:251–62.
52. Wang XG, Chen ZG, Mishra AK, Silva A, Ren WH, Pan ZG, et al. Chemotherapy-induced differential cell cycle arrest in B-cell lymphomas affects their sensitivity to Wee1 inhibition. Haematologica 2018;103:466–76.
53. Chen Z, Ranganath S, Viboolsittiseri SS, Eder MD, Chen X, Elos MT, et al. AID-initiated DNA lesions are differentially processed in distinct B cell populations. J Immunol 2014;193:5545–56.
54. Ran FA, Hsu PD, Wright J, Agarwala V, Scott DA, Zhang F. Genome engineering using the CRISPR-Cas9 system. Nat Protoc 2013;8: 2281–308.
55. Salvador LA, Park H, Al-Awadhi FH, Liu Y, Kim B, Zeller SL, et al. Modulation of activity profiles for largazole-based HDAC inhibitors through alteration of prodrug properties. ACS Med Chem Lett 2014;5: 905–10.
56. Chen QY, Chaturvedi PR, Luesch H. Process development and scale-up total synthesis of largazole, a potent class I histone deacetylase inhibitor. Org Process Res Dev 2018;22:190–9.
57. West AC, Johnstone RW. New and emerging HDAC inhibitors for cancer treatment. J Clin Invest 2014;124:30–9.
58. Ferris RL, Blumenschein G Jr, Fayette J, Guigay J, Colevas AD, Licitra L, et al. Nivolumab for recurrent squamous-cell carcinoma of the head and neck. N Engl J Med 2016;375:1856–67.
59. Zou W, Wolchok JD, Chen L. PD-L1 (B7-H1) and PD-1 pathway blockade for cancer therapy: mechanisms, response biomarkers, and combinations. Sci Transl Med 2016;8:328rv4.
60. Green MR, Monti S, Rodig SJ, Juszczynski P, Currie T, O'Donnell E, et al. Integrative analysis reveals selective 9p24.1 amplification, increased PD-1 ligand expression, and further induction via JAK2 in nodular sclerosing Hodgkin lymphoma and primary mediastinal large B-cell lymphoma. Blood 2010;116:3268–77.
61. Steidl C, Shah SP, Woolcock BW, Rui L, Kawahara M, Farinha P, et al. MHC class II transactivator CIITA is a recurrent gene fusion partner in lymphoid cancers. Nature 2011;471:377–81.
62. Zaretsky JM, Garcia-Diaz A, Shin DS, Escuin-Ordinas H, Hugo W, Hu-Lieskovan S, et al. Mutations associated with acquired resistance to PD-1 blockade in melanoma. N Engl J Med 2016;375:819–29.
63. Wang X, Schoenhals JE, Li A, Valdecanas DR, Ye H, Zang F, et al. Suppression of type I IFN signaling in tumors mediates resistance to anti-PD-1 treatment that can be overcome by radiotherapy. Cancer Res 2017;77: 839–50.
64. Rodig SJ, Gusenleitner D, Jackson DG, Gjini E, Giobbie-Hurder A, Jin C, et al. MHC proteins confer differential sensitivity to CTLA-4 and PD-1 blockade in untreated metastatic melanoma. Sci Transl Med 2018;10:pii: eaar3342.
65. Li L, Dong M, Wang XG. The implication and significance of beta 2 microglobulin: a conservative multifunctional regulator. Chin Med J 2016;129:448–55.
66. West AC, Mattarollo SR, Shortt J, Cluse LA, Christiansen AJ, Smyth MJ, et al. An intact immune system is required for the anticancer activities of histone deacetylase inhibitors. Cancer Res 2013;73:7265–76.
67. West AC, Smyth MJ, Johnstone RW. The anticancer effects of HDAC inhibitors require the immune system. Oncoimmunology 2014;3: e27414.
68. Tao R, de Zoeten EF, Ozkaynak E, Chen C, Wang L, Porrett PM, et al. Deacetylase inhibition promotes the generation and function of regulatory T cells. Nat Med 2007;13:1299–307.
69. Jiang Y, Ortega-Molina A, Geng H, Ying HY, Hatzi K, Parsa S, et al. CREBBP inactivation promotes the development of HDAC3-dependent lymphomas. Cancer Discov 2017;7:38–53.
70. Dong H, Strome SE, Salomao DR, Tamura H, Hirano F, Flies DB, et al. Tumor-associated B7-H1 promotes T-cell apoptosis: a potential mechanism of immune evasion. Nat Med 2002;8:793–800.
71. Woods DM, Sodre AL, Villagra A, Sarnaik A, Sotomayor EM, Weber J. HDAC inhibition upregulates PD-1 ligands in melanoma and augments immunotherapy with PD-1 blockade. Cancer Immunol Res 2015;3: 1375–85.
72. Zinzani PL, Ribrag V, Moskowitz CH, Michot JM, Kuruvilla J, Balakumaran A, et al. Safety and tolerability of pembrolizumab in patients with relapsed/refractory primary mediastinal large B-cell lymphoma. Blood 2017;130: 267–70.
73. Tang H, Liang Y, Anders RA, Taube JM, Qiu X, Mulgaonkar A, et al. PD-L1 on host cells is essential for PD-L1 blockade-mediated tumor regression. J Clin Invest 2018;128:580–8.

Published OnlineFirst June 24, 2019; DOI: 10.1158/2326-6066.CIR-18-0875

Cancer Immunology Research

Histone Deacetylase Inhibition Sensitizes PD1 Blockade–Resistant B-cell Lymphomas

Xiaoguang Wang, Brittany C. Waschke, Rachel A. Woolaver, et al.

Cancer Immunol Res 2019;7:1318-1331. Published OnlineFirst June 24, 2019.